

## Article

# Experimental Investigation on Ice–Aluminum Interface Adhesion Strength under Heating Conditions

Yusong Wang <sup>1</sup>, Chengxiang Zhu <sup>1</sup>, Ke Xiong <sup>1,2</sup> and Chunling Zhu <sup>1,2,\*</sup>

<sup>1</sup> College of Aerospace Engineering, Nanjing University of Aeronautics and Astronautics, Nanjing 210016, China; yswang1873@nuaa.edu.cn (Y.W.); cxzhu@nuaa.edu.cn (C.Z.); kxiong@nuaa.edu.cn (K.X.)

<sup>2</sup> State Key Laboratory of Mechanics and Control of Mechanical Structures, Nanjing University of Aeronautics & Astronautics, Nanjing 210016, China

\* Correspondence: clzhu@nuaa.edu.cn; Tel.: +86-025-84896667

**Abstract:** Ice accumulation on airfoils and engines seriously endangers flight safety. The design of anti-icing/de-icing systems calls for an accurate measurement of the adhesion strength between ice and substrates. In this research, a test bench for adhesion strength measurement is designed and built. Its reliability and accuracy are verified by the calibration. The adhesion strength is first measured at different loading speeds and freezing times, and the most suitable values are determined based on the results. Then, the variation in adhesion strength with heating temperatures at different initial substrate temperatures and different heating powers is investigated. Parameter AW is defined to evaluate the heating power from the point of view of energy consumption and adhesion strength. As a result, the loading speed and the freezing time are determined to be 0.5 mm/s and 90 min, respectively. The adhesion strength degrades as the heating temperature increases. As the initial temperature drops, the adhesion strength decreases more slowly. Furthermore, the temperature of WAS (Weak Adhesion State) under heating varies with the initial temperature. Heating with a high power will yield more reduction in adhesion strength for the same temperature increase. The values of AW illustrate that a medium power heating is more favorable to reduce the adhesion strength with a low energy consumption.



**Citation:** Wang, Y.; Zhu, C.; Xiong, K.; Zhu, C. Experimental Investigation on Ice–Aluminum Interface Adhesion Strength under Heating Conditions. *Aerospace* **2024**, *11*, 152. <https://doi.org/10.3390/aerospace11020152>

Academic Editors: Hirotaka Sakaue and Xiaobin Shen

Received: 15 January 2024

Revised: 5 February 2024

Accepted: 9 February 2024

Published: 14 February 2024



**Copyright:** © 2024 by the authors. Licensee MDPI, Basel, Switzerland. This article is an open access article distributed under the terms and conditions of the Creative Commons Attribution (CC BY) license (<https://creativecommons.org/licenses/by/4.0/>).

**Keywords:** aircraft de-icing; adhesion strength; experimental setup; initial temperature; heating power

## 1. Introduction

When an aircraft encounters cold cloud conditions during a flight, icing can occur on the surface of the skin. Aircraft icing causes overall lift falling and an increase in drag, which leads to a serious threat to flight safety [1,2]. Therefore, research on effective anti-/de-icing systems requires considerable attention in aircraft design. Currently, there are several well-established anti-icing/de-icing systems, including the electrothermal system, electro-impulse system, and hot-air system [3–5]. Meanwhile, some new technologies, such as plasma jets, icephobic surfaces, and hybrid systems, have been remarkably developed [6–8]. The most typical hybrid de-icing system is the electrothermal–mechanical de-icing system. The interface is first partially melted by heating, and the ice is subsequently dislodged by mechanical force [9,10]. The major advantage of the hybrid de-icing system is that it takes into account the optimization of de-icing efficiency and energy consumption.

Regardless of the anti-icing/deicing technology used, the critical problem of the anti-icing and deicing of aircraft lies in the study of the adhesion between ice and skin. Therefore, ice adhesion has been broadly studied by researchers. In terms of theoretical research, scholars are committed to studying adhesion mechanisms. Petrenko and Whitworth explained the adhesion mechanism between ice and substrates from the molecular perspective [11]. The mechanisms were roughly divided into three categories: covalent bonds or chemical

bonds, Van Dehwa, and ionic power. Knuth et al. interpreted the adhesion of ice mainly as a mechanical connection theory. This theory suggested that, when ice entered a structure such as a groove or a hole on the surface of an object, it formed an “anchor”-like structure that connected the ice to the substrate. Based on this theory, he proposed a mathematical model for shear adhesion strength prediction [12]. Derjagin presented the electrostatic adhesion theory, which believed that there was a mutual attraction between the ice and the substrate with the main force of electrostatic gravity [13]. Guy Fortin also introduced an adhesion model based on this theory [14]. Frederic Guerin considered the existence of a liquid-like layer (LLL) between the ice and the substrate, with properties intermediate to those of ice and water. He put forward a formula for calculating the adhesion strength, which took into account the surface structure, surface energy, and medium volume diameter (MVD), etc. [15].

Although some theoretical studies have been conducted, a theoretical model that takes all factors into account has not yet been formulated due to the large number of factors affecting ice adhesion. On the other hand, since some of the parameters in the theoretical model are also uncertain, it is difficult to calculate ice adhesion parameters directly from the theoretical model without any experiment [16]. Therefore, experimental studies become essential for ice adhesion. The shear adhesion force between the substrate and the ice layer is the main factor affecting the ice–substrate separation [17]. For most de-icing systems, especially mechanical de-icing systems, including electric impulse de-icing systems and piezoelectric de-icing systems, etc., ice detachment is caused by the shear force [18]. Most of the experimental studies by scholars have measured shear adhesion force or shear adhesion strength. In these experiments, the ice will eventually detach in the shear direction. The centrifuge adhesion test (CAT) and the direct mechanical test are the two most commonly used testing methods. The Anti-icing Materials International Laboratory (AMIL) introduced the centrifuge adhesion test (CAT) to study adhesion force in 2005, which utilized centrifuge force to remove the ice [19]. Due to the similar working principle, this method was often used to study the adhesion of rotorcraft surfaces [20]. The adhesion strength of superhydrophobic surfaces was evaluated by Kulinich using this method [21]. Stefania studied the atmosphere ice shedding properties on helicopter blades with the centrifuge method [22]. Ice-coating samples were spun in a centrifuge device by Zaid. This research found that icephobicity was not linked to hydrophobicity [23]. Brouwers et al. used the instrumented CAT (ICAT) to study the ice adhesion, which involved an airfoil and impact ice in the test [24]. In this study, centrifugal force was increased by the continuous accumulation of ice, which is different from the previous approach of increasing the rotation speed. However, the issues of accurate capture at the moment of ice shedding and the integrity of the sample cannot be avoided for methods based on centrifuge force.

Apart from the CAT, the direct push/pull method has also been adopted by many scholars to measure adhesion strength. In this approach, the interface between the ice and the substrate is separated by force applied directly to the ice sample. A push test was used to investigate the relationship between water wettability and ice adhesion by Adam J [25]. Ge pushed the ice using a needle to evaluate the anti-icing property of the superhydrophobic surface [26]. Kevin evaluated the forces that dislodge ice of different scales using the push method. The results showed that there was a critical bonded length at which a transition between the strength-controlled and toughness-controlled failure mode occurred [27]. Recently, Wang designed a new setup to measure the adhesive shear strength of impact ice on different substrates in icing wind [28]. Compared to the centrifugal method, the direct mechanical test proves to be more cost-effective, time-efficient, and valid. Although centrifugal tests usually yield more consistent results, many researchers prefer to use direct push/pull methods due to their advantages. In addition to the centrifugal and direct push/pull methods, there are some niche methods used by other scholars. Sarkar and Javan-Mashmool investigated ice adhesion with beam tests [29,30]. In their tests, beam substrates were deformed to stress the ice–substrate interface. Archer and Gupta only

published the laser spallation technique in one paper. In their experiment, they used a laser to heat the back side of an iced substrate [31].

Building on the above studies, many scholars have conducted experimental analyses and theoretical studies on icing adhesion. However, none of the above studies addressed ice adhesion under heating conditions. Due to the wide application and good prospect of electrothermal anti-/de-icing systems, it is imperative to study ice adhesion properties in the case of substrate heating. Especially for electro-thermal-mechanical de-icing systems, the nature of ice adhesion after heating will determine the working load and duration of the mechanical de-icing system. A thorough understanding of ice adhesion under heating conditions can improve the de-icing effect and reduce the energy consumption of composite de-icing systems. To tackle this problem, Zhang conducted preliminary research for composite materials, in which ice adhesion forces were measured under various heating temperatures, heating voltages, and heating times. The aluminum substrate was not included in his study [32]. It was found that more energy consumption leads to more adhesion strength reduction. However, from the point of view of energy saving, we need to find a balance between energy consumption and adhesion strength degradation. This issue is currently unexplored.

In this article, we design and establish an experimental device to measure the shear force between ice and an aluminum substrate. The accuracy of experiments is ensured by some scientific approaches. A series of experiments are carried out to test the shear adhesion strength under different heating parameters. A dimensionless parameter is defined to find a trade-off between energy cost and adhesion strength decrease.

## 2. Experimental Setup

### 2.1. Experimental Design

The direct-force test typified by the push method is one of the most reliable approaches to determining the adhesive strength between ice and substrate. We devised an experimental setup on the basis of this principle. The panorama is shown in Figure 1.

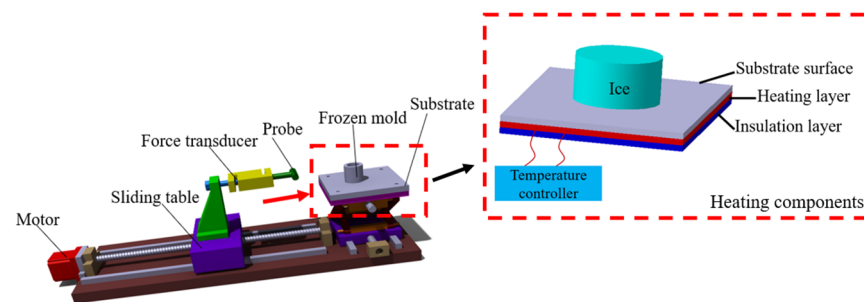


**Figure 1.** The panorama of the experimental setup.

Ice is frozen in a mold on the aluminum plate first. Then, the sliding table is driven by the motor to move toward the ice. Naturally, the force transducer and the probe also move to push the mold and ice to slide. At the moment of ice detachment from the substrate, the sensor indication is the adhesion shear force. The shear strength can be calculated by dividing the adhesion force by the contact area between the ice and aluminum plate:

$$\tau = \frac{F}{A}, \quad (1)$$

where  $\tau$  is the adhesion shear strength,  $F$  is the adhesion shear force, and  $A$  is the contact area between the ice and aluminum plate.

As shown in Figure 1, the heating components are composed of a substrate surface, heating layer, and insulation layer. The insulation layer is to stop the heat from traveling in other directions. The heating layer is embedded in the middle of the substrate surface and

insulation layer. The heating temperature can be changed by the controller. All substrate surfaces were sanded with 1000 grit sandpaper to ensure a similar surface roughness.

## 2.2. Calibration of the Experimental Setup

In order to verify the accuracy of this test platform and experimental method, the friction force, which is also the interface shear force, was measured in this paper. The friction coefficient between the interfaces was inversely calculated by the friction force, and the measured results were compared with those obtained from the standard friction test method by ramp.

Two aluminum plates with different roughness were selected as the substrate for the calibration test, and two samples with different weights and materials were also adopted. A digital optical microscope was used to observe the real surface morphology and measure the roughness. The microscope can take thousands of photographs continuously in the height direction, thus obtaining height information about the surface topography. The surface roughness can then be calculated. It was assessed in this research by the means of the arithmetic mean deviation of the profile, abbreviated as  $R_a$ . The range of each measurement was  $0.5 \text{ mm} \times 0.5 \text{ mm}$ . For each sample, 5 test regions were selected for testing and the results were averaged. The data of the substrate and sample pieces are shown in Tables 1 and 2. Four sets of experiments were conducted, each on the experimental platform of this paper and the standard friction test bench, respectively.

**Table 1.** The data of substrates for calibration.

Series Number	Material	Roughness ( $R_a$ )/ $\mu\text{m}$
1	Aluminum	2.8
2	Aluminum	1.2

**Table 2.** The data of samples for calibration.

Series Number	Material	Mass (m)/Kg
1	Lead	1.14
2	Iron	0.978

For the standard friction test method by ramp, the critical angle of inclination was measured. The sliding friction coefficient between the sample and the substrate was calculated by Equation (2). For the setup in this research, the probe was driven by the motor to push the sample to slide on the substrate. The sensor signal was collected during stable sliding, which is the sliding friction between the sample and the substrate. The sliding friction coefficient was calculated by Equation (3).

$$\mu_1 = \tan(\theta), \quad (2)$$

where  $\mu_1$  is the sliding friction coefficient with the ramp method and  $\theta$  is the critical inclination angle while sliding.

$$\mu_2 = \frac{T}{mg}, \quad (3)$$

where  $\mu_2$  is the sliding friction coefficient with the setup in this research,  $T$  is the push force while sliding stably, and  $g$  is the gravitational acceleration.

## 3. Results and Discussion

### 3.1. Calibration Results

Table 3 shows the results of the standard friction test. The critical inclination angle is the average of multiple measurements. In the test serial number “1–2”, 1 refers to the substrate serial number in Table 1, the data of substrates for calibration, and 2 refers to the

sample serial number in Table 2. The results measured with the adhesion measurement platform developed in this paper are listed in Table 4.

**Table 3.** The results of the standard friction test.

Series Number	Critical Inclination ( $\theta$ )/°	Friction Coefficient ( $\mu_1$ )
1-1	30.94	0.6
1-2	25.05	0.47
2-1	20.21	0.37
2-2	14.53	0.26

**Table 4.** The results of adhesion test developed in this paper.

Series Number	Push Force (T)/N	Friction Coefficient ( $\mu_2$ )
1-1	6.1	0.55
1-2	4.65	0.49
2-1	3.95	0.35
2-2	2.55	0.27

Figure 2 illustrates the comparison of the friction coefficients measured by the above two methods. It can be seen that the difference between them is small, with an overall error of about 5%. This proves that the measurement rig established in this project is highly accurate and reliable in measuring interface forces such as friction and shear adhesion force.

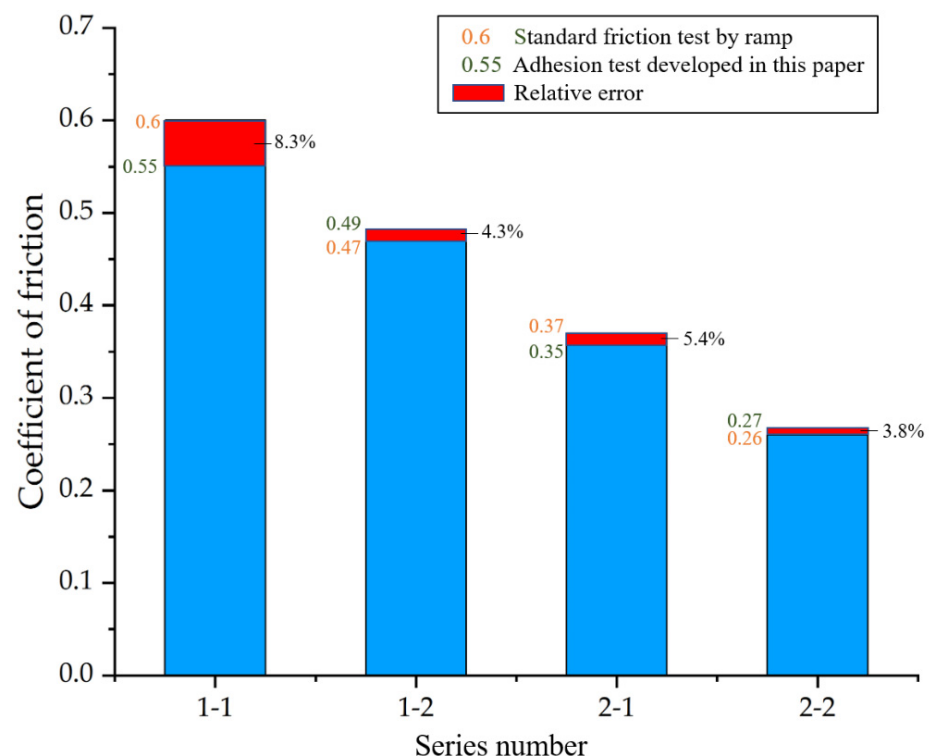


**Figure 2.** Comparison of the friction coefficients.

### 3.2. Determination of Loading Speed

The loading speed is achieved by changing the excitation frequency of the motor. In this set of experiments, the substrate surface roughness is about  $0.124 \mu\text{m}$  and the substrate temperature is  $-10 \text{ }^\circ\text{C}$ . Each loading speed was tested at least three times.

Figure 3 demonstrates the adhesion strength at different loading speeds. The loading speed has a small effect on the absolute magnitude of the adhesion strength, which almost

remains between 0.2 MPa and 0.25 MPa. However, it is obvious that the data dispersion is larger at a high loading speed. This means that the ice ductility does not change significantly in this loading speed range, but the data acquisition frequency is limited. When the loading speed is too large, the acquired signal does not exactly correspond to the moment of ice shedding, thus resulting in a large scatter of data. On the other hand, due to the limitation of the experimental equipment, the motor will work unstably when the loading speed is less than 0.1 mm/s. Therefore, in order to improve the accuracy of the experiment, the loading speed of subsequent experiments is determined to be 0.5 mm/s.

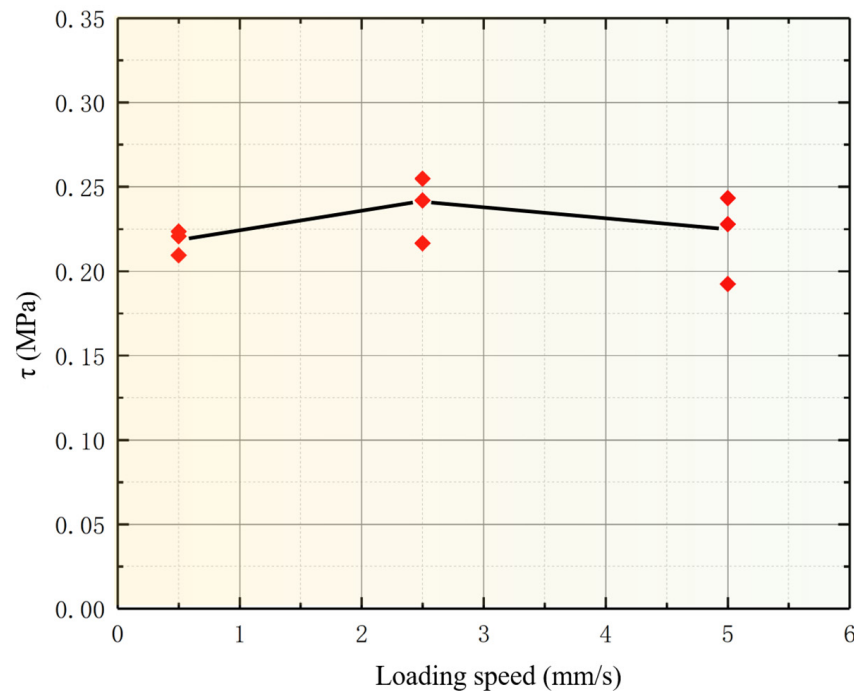


**Figure 3.** Adhesion strength at different loading speeds.

### 3.3. Determination of Freezing Time

Freezing time is defined as the length of time from water injection to mold to ice shedding. The cooling time of the substrate is not included. In this group of experiments, the substrate surface roughness is about  $0.14 \mu\text{m}$  and the substrate temperature is  $-10 \text{ }^\circ\text{C}$ . Similarly, each loading speed was tested at least three times to reduce error.

As Figure 4 shows, the adhesion strength grows as the freezing time increases, but the growth rate gradually slows down. When the freezing time increases from 40 min to 90 min, the growth rate is  $0.8 \text{ KPa}/\text{min}$ ; when it increases from 180 min to 720 min, the growth rate decreases to  $0.1 \text{ KPa}/\text{min}$ . As the freezing time rises, the residual stress between the ice and the substrate gradually diminishes. The connection between them becomes more stable. When the time is long enough, the residual stress tends to zero and the adhesion strength will also stabilize. Taking into account the above results and experimental efficiency, we set the freezing time for the subsequent experiments at 90 min.

### 3.4. Effect of Initial Temperature on Adhesion Strength under Heating Conditions

For different substrate temperatures, the adhesion strength is first measured before heating. As Figure 5 shows, box plots were used to achieve a high data quality. The  $1.5 \times \text{IQR}$  rule was selected (interquartile range IQR multiplied by 1.5 and added to the third quartile or subtracted from the first quartile) as an established statistical tool. It was found that the means of adhesion strength decreases as the substrate temperature falls without heating. At lower temperatures, water freezes rapidly upon contact with the substrate, while at higher temperatures, water partially penetrates into the surface

microstructure before freezing, which enhances the anchoring effect between the ice and substrate. It is similar to the transition from Cassie-state to Wenzel-state. In addition, Figure 6 depicts the topography of the bottom surface after ice was removed. At  $-10\text{ }^{\circ}\text{C}$ , the surface was smooth and intact. Interestingly, a few circles of stripes appeared on the surface at  $-20\text{ }^{\circ}\text{C}$ , which means that the water was gradually frozen in the order of contact with the surface. The surface discontinuity caused by these stripes would also contribute to a decline in adhesion strength.

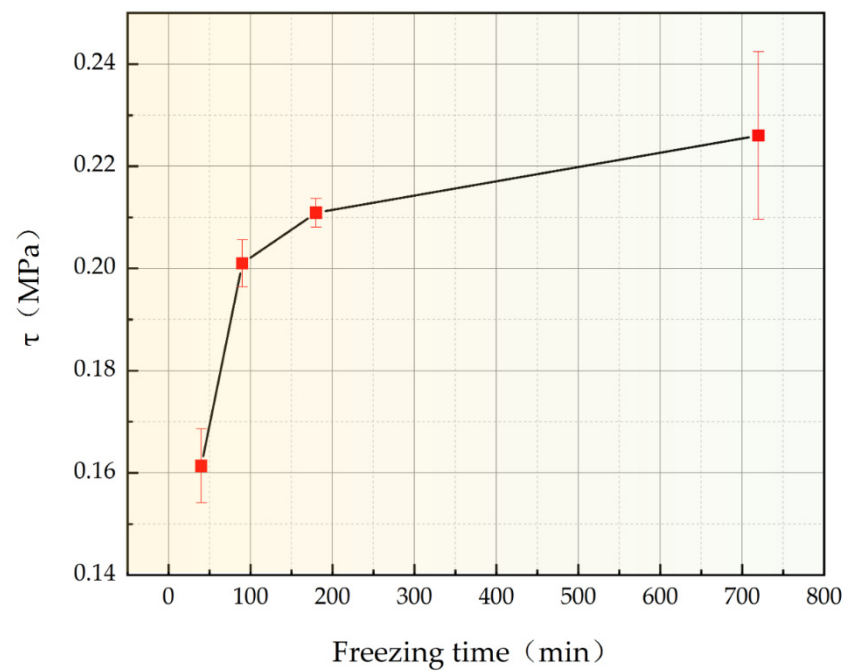


Figure 4. Adhesion strength at different freezing times.

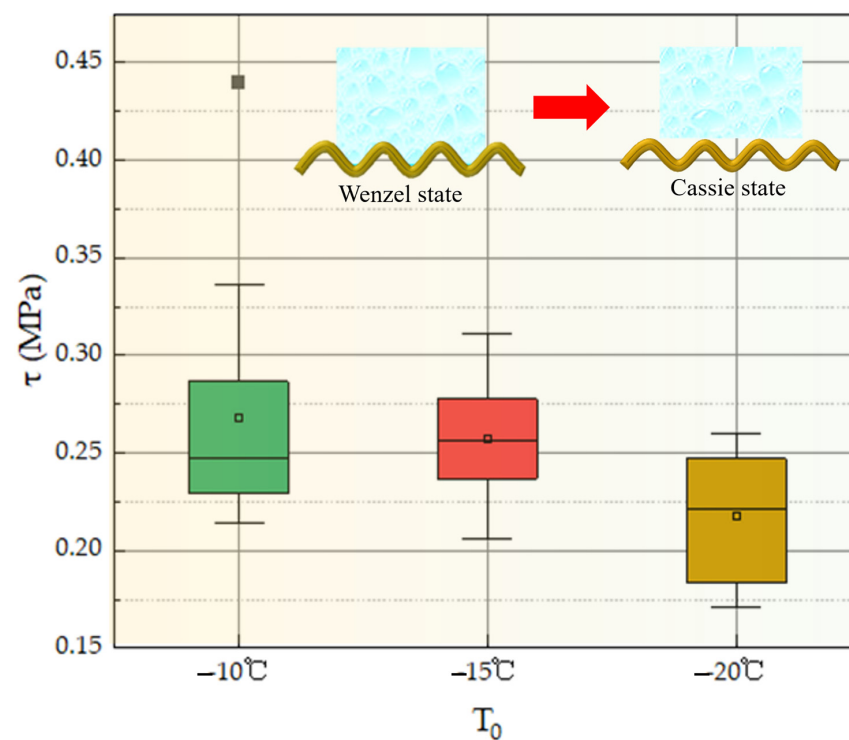
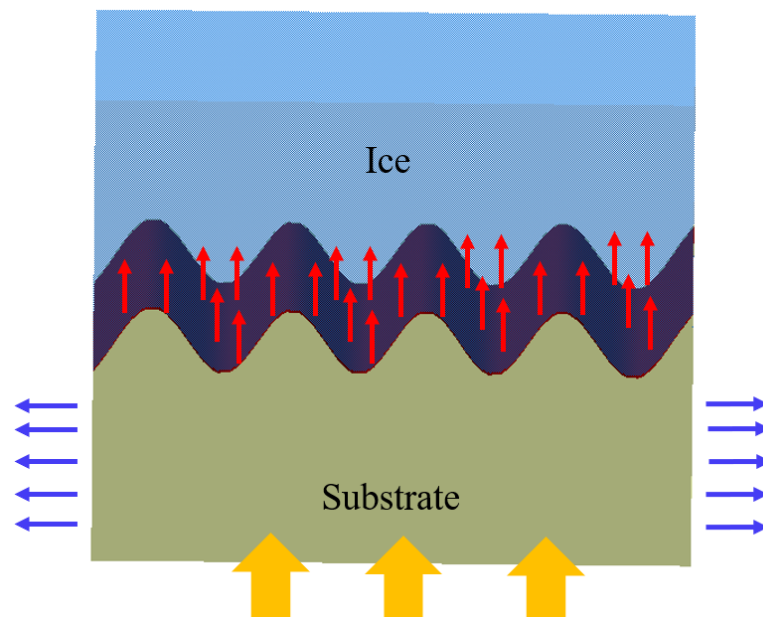


Figure 5. Adhesion strength at different substrate temperatures before heating.



there was less ice or even no ice in the substrate surface microstructure at the lower initial temperature compared to the higher initial temperature. Thus, at a high initial temperature, more of the heat energy would be used to melt the ice; at a low initial temperature, less of the ice would be melted and more heat energy would be dissipated, as shown in Figure 8. Moreover, at a low initial temperature, the substrate had a slower temperature rise under heating. For the same temperature increase, this means that consuming more energy did not have a significant effect on the reduction in adhesion strength.



**Figure 8.** Utilization of the heat energy.

To better describe the relative strength of adhesion, we define the adhesion state with an adhesion strength of less than 0.1 MPa as a weak adhesion state (WAS). As shown in Figure 7, the temperature of WAS varied from about  $-4\text{ }^{\circ}\text{C}$  to  $-7\text{ }^{\circ}\text{C}$  and then  $-9\text{ }^{\circ}\text{C}$  when the initial temperature changed from  $-10\text{ }^{\circ}\text{C}$  to  $-15\text{ }^{\circ}\text{C}$  and then  $-20\text{ }^{\circ}\text{C}$ . It was apparent that more energy would be consumed at a low initial temperature to reach the WAS, although the adhesion strength was lower at a low initial temperature without heating. Meanwhile, the results implied that it was not necessary to heat the substrate to above zero temperature when using an electric heating system (especially an electric–mechanical coupling system) for de-icing. Even when the initial temperature was low, it was enough to heat the surface to  $-10\text{ }^{\circ}\text{C}$ . The ice could be easily removed by aerodynamic or mechanical forces when the adhesion was in the WAS.

### 3.5. Effect of Heating Power on Adhesion Strength

In order to investigate the effect of the heating rate on the adhesion strength, the substrate was heated by different powers (10 W, 30 W, and 50 W). Figure 9 demonstrates the results at three different levels of power. Since the different powers were not applied on the same substrate, there was a slight difference in their initial adhesion strengths when unheated ( $T_h = -10\text{ }^{\circ}\text{C}$ ), although the pretreatment was the same for each substrate. With the same temperature rise, the higher the heating power, the more the adhesion strength decreased, although the heating time was shorter. The slopes were  $-0.014\text{ MPa}/^{\circ}\text{C}$ ,  $-0.028\text{ MPa}/^{\circ}\text{C}$ , and  $-0.032\text{ MPa}/^{\circ}\text{C}$  for 10 W, 30 W, and 50 W, respectively. For the power of 10 W, the adhesion strength was about 0.2 MPa at  $-4\text{ }^{\circ}\text{C}$ , which had not yet reached the WAS. Therefore, a heating power of 10 W was not sufficient to reduce the adhesion strength.

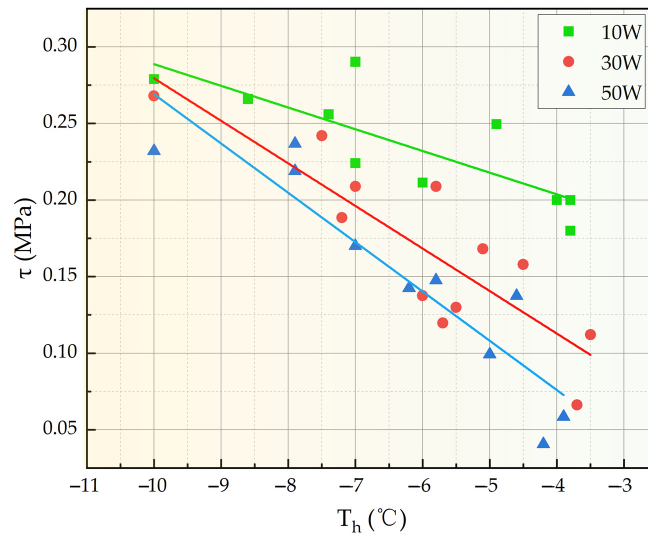


Figure 9. Adhesion strength at different heating temperature for various heating powers.

It was known that a higher power would bring more energy consumption. Therefore, both the energy consumption and adhesion strength reduction should be taken into account when selecting the heating power. A dimensionless parameter *AW* considering the above two factors was defined by Equation (4), which characterized the adhesion weakening per unit of energy consumption.

$$AW = \frac{\tau_0 - \tau_h}{P \cdot t} \cdot V \tag{4}$$

where  $\tau_0$  and  $\tau_h$  are the adhesion strength before and after heating, respectively. *P* is the heating power. *t* is the heating time. *V* is the volume of the ice sample, which could be easily calculated by the bottom area and height of cylindrical ice.

Figure 10 depicts the results of *AW* at different heating powers. The values of *AW* were 2.94, 3.07, and 2.18 for 10 W, 30 W, and 50 W, respectively. *AW* at 30 W was the largest, followed by 10 W and 50 W. A heating power of 50 W could bring about degradation of the adhesion strength in a short time, but it was not energy saving at all. Therefore, from the point of view of energy optimization, a medium power (i.e., 30 W) should be selected for heating to reduce the adhesion strength.

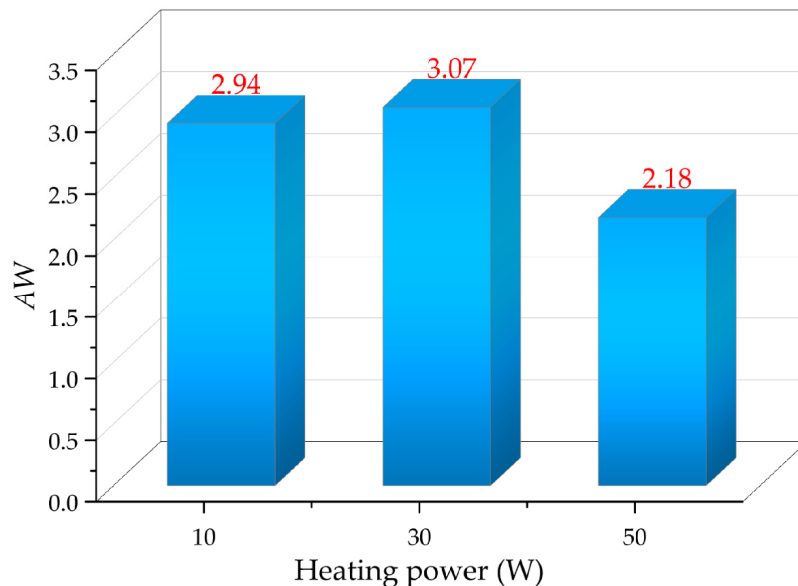


Figure 10. Adhesion weakening at various heating powers.

#### 4. Conclusions

In this study, a high-precision adhesion test rig is established and adhesion strength under heating conditions is investigated. The experimental setup is calibrated by comparing the measurement results of the friction coefficient with the standard ramp method. The overall error of about 5% between the two methods reveals that the rig established in this project is highly accurate and reliable in measuring interface forces such as friction and shear adhesion force. The variation in adhesion strength with heating temperature at different initial temperatures and different heating powers is observed. The following conclusions are drawn:

- (1) The loading speed and the freezing time are determined to be 0.5 mm/s and 90 min, respectively, by measuring the shear strength under different conditions.
- (2) The adhesion strength degrades as the heating temperature increases. As the initial temperature drops, the adhesion strength decreases slower.
- (3) The weak adhesion state (WAS) is defined to describe the adhesion. The temperature of WAS under heating varies with the initial temperature. A higher heating power reduces the adhesion strength more with the same temperature rise.
- (4) The dimensionless parameter  $AW$  is introduced to take the energy consumption and adhesion weakening into account. The values of  $AW$  suggest that a medium power should be selected for heating to reduce the adhesion strength.

Based on the research results of this paper, energy-efficient and reliable electro-thermal or electro-mechanical hybrid de-icing systems can be developed to cope with de-icing needs.

**Author Contributions:** Conceptualization, Y.W. and C.Z. (Chunling Zhu); methodology, Y.W.; validation, Y.W. and K.X.; formal analysis, Y.W.; investigation, Y.W. and C.Z. (Chengxiang Zhu); resources, C.Z. (Chunling Zhu); data curation, Y.W. and C.Z. (Chengxiang Zhu); writing—original draft preparation, Y.W.; writing—review and editing, Y.W., C.Z. (Chengxiang Zhu), K.X. and C.Z. (Chunling Zhu); visualization, K.X.; supervision, C.Z. (Chunling Zhu); project administration, K.X. and C.Z. (Chunling Zhu); funding acquisition, C.Z. (Chunling Zhu). All authors have read and agreed to the published version of the manuscript.

**Funding:** This research is funded by the National Natural Science Foundation of China (Grant No. 11832012), the Fundamental Research Funds for the Central Universities (Grant No. NS2019010) and the National Natural Science Foundation of China (Grant No. 12227802).

**Data Availability Statement:** Data are contained within the article.

**Acknowledgments:** The authors wish to acknowledge the staffs in Icing Wind Tunnel Laboratory of Nanjing University of Aeronautics and Astronautics in China for their efforts in experiments.

**Conflicts of Interest:** The authors declare no conflicts of interest.

#### References

1. Lampton, A.; Valasek, J. Prediction of icing effects on the lateral/directional stability and control of light airplanes. *Aerosp. Sci. Technol.* **2012**, *23*, 305–311. [[CrossRef](#)]
2. Cao, Y.; Tan, W.; Wu, Z. Aircraft icing: An ongoing threat to aviation safety. *Aerosp. Sci. Technol.* **2018**, *75*, 353–385. [[CrossRef](#)]
3. Bennani, L.; Trontin, P.; Radenac, E. Numerical Simulation of an Electrothermal Ice Protection System in Anti-Icing and Deicing Mode. *Aerospace* **2023**, *10*, 75. [[CrossRef](#)]
4. Wang, Y.; Guo, T.; Li, K.; Zhu, C.; Du, Q. Research on the dual-channel electro-impulse de-icing system of aircrafts. *Proc. Inst. Mech. Eng. Part G J. Aerosp. Eng.* **2022**, *236*, 2315–2326. [[CrossRef](#)]
5. Planquart, P.; Vanden Borre, G.; Buchlin, J.-M. Experimental and numerical optimization of a wing leading edge hot air anti-icing system. In Proceedings of the 43rd AIAA Aerospace Sciences Meeting and Exhibit, Reno, NV, USA, 10–13 January 2005; p. 1277.
6. Wang, P.; Yao, T.; Li, Z.; Wei, W.; Xie, Q.; Duan, W.; Han, H. A superhydrophobic/electrothermal synergistically anti-icing strategy based on graphene composite. *Compos. Sci. Technol.* **2020**, *198*, 108307. [[CrossRef](#)]
7. Zhang, Z.; Lusi, A.; Hu, H.; Bai, X.; Hu, H. An experimental study on the detrimental effects of deicing fluids on the performance of icephobic coatings for aircraft icing mitigation. *Aerosp. Sci. Technol.* **2021**, *119*, 107090. [[CrossRef](#)]
8. Kolbakir, C.; Hu, H.; Liu, Y.; Hu, H. An experimental study on different plasma actuator layouts for aircraft icing mitigation. *Aerosp. Sci. Technol.* **2020**, *107*, 106325. [[CrossRef](#)]

9. Al-Khalil, K. Thermo-Mechanical Expulsive Deicing System—TMEDS. In Proceedings of the Aiaa Aerospace Sciences Meeting & Exhibit, Reno, NV, USA, 8–11 January 2013.
10. Strobl, T.; Storm, S.; Thompson, D.; Hornung, M.; Thielecke, F. Feasibility Study of a Hybrid Ice Protection System. *J. Aircr.* **2015**, *52*, 2064–2076. [[CrossRef](#)]
11. Petrenko, V.F.; Whitworth, R.W. *Physics of Ice*; OUP: Oxford, UK, 1999.
12. Knuth, T.D. Ice Adhesion Strength Modeling Based on Surface Morphology Variations. Master's Thesis, The Pennsylvania State University, State College, PA, USA, 2015.
13. Deriagin, B.V.; Krotova, N.; Smilga, V.d.P. *Adhesion of Solids*; Springer: Berlin/Heidelberg, Germany, 1978.
14. Fortin, G.; Perron, J. Ice adhesion models to predict shear stress at shedding. *J. Adhes. Sci. Technol.* **2012**, *26*, 523–553. [[CrossRef](#)]
15. Guerin, F.; Laforte, C.; Farinas, M.-I.; Perron, J. Analytical model based on experimental data of centrifuge ice adhesion tests with different substrates. *Cold Reg. Sci. Technol.* **2016**, *121*, 93–99. [[CrossRef](#)]
16. Qin, L.; Du, W.; Cipiccia, S.; Bodey, A.J.; Rau, C.; Mi, J. Synchrotron X-ray operando study and multiphysics modelling of the solidification dynamics of intermetallic phases under electromagnetic pulses. *Acta Mater.* **2024**, *265*, 119593. [[CrossRef](#)]
17. Scavuzzo, R.J.; Chu, M.L. *Structural Properties of Impact Ices Accreted on Aircraft Structures*; NASA: Washington, DC, USA, 1987.
18. Huang, Y.; Yi, X.; Liu, Q.; Ni, Z.; Pan, P.; Zhang, Y. *Simulation of Electro-Impulse De-Icing Process Based on an Improved Ice Shedding Criterion*; Springer: Singapore, 2023. [[CrossRef](#)]
19. Laforte, C.; Beisswenger, A. Icephobic material centrifuge adhesion test. In Proceedings of the 11th International Workshop on Atmospheric Icing of Structures, IWAIS, Montreal, QC, Canada, 12–16 June 2005; pp. 12–16.
20. Morelli, M.; Guardone, A. A simulation framework for rotorcraft ice accretion and shedding. *Aerosp. Sci. Technol.* **2021**, *129*, 107157. [[CrossRef](#)]
21. Kulinich, S.; Farzaneh, M. On ice-releasing properties of rough hydrophobic coatings. *Cold Reg. Sci. Technol.* **2011**, *65*, 60–64. [[CrossRef](#)]
22. Tarquini, S.; Antonini, C.; Amirfazli, A.; Marengo, M.; Palacios, J. Investigation of ice shedding properties of superhydrophobic coatings on helicopter blades. *Cold Reg. Sci. Technol.* **2014**, *100*, 50–58. [[CrossRef](#)]
23. Turnbull, B.; Choy, K.L.; Pandis, C.; Liu, J.; Hou, X.; Choi, K.S. Performance and durability tests of smart icephobic coatings to reduce ice adhesion. *Appl. Surf. Sci.* **2017**, *407*, 555–564. [[CrossRef](#)]
24. Brouwers, E.W.; Peterson, A.A.; Palacios, J.L.; Centolanza, L.R. Ice adhesion strength measurements for rotor blade leading edge materials. In Proceedings of the 67th American Helicopter Society International Annual Forum 2011, Virginia Beach, VA, USA, 3–5 May 2011; pp. 3011–3023.
25. Meuler, A.J.; Smith, J.D.; Varanasi, K.K.; Mabry, J.M.; McKinley, G.H.; Cohen, R.E. Relationships between water wettability and ice adhesion. *ACS Appl. Mater. Interfaces* **2010**, *2*, 3100–3110. [[CrossRef](#)]
26. Ge, L.; Ding, G.; Wang, H.; Yao, J.; Cheng, P.; Wang, Y. Anti-icing property of superhydrophobic octadecyltrichlorosilane film and its ice adhesion strength. *J. Nanomater.* **2013**, *2013*, 278936. [[CrossRef](#)]
27. Golovin, K.; Dhyani, A.; Thouless, M.; Tuteja, A. Low-interfacial toughness materials for effective large-scale deicing. *Science* **2019**, *364*, 371–375. [[CrossRef](#)] [[PubMed](#)]
28. Yusong, W.; Ke, X.; Chunling, Z.; Chengxiang, Z.; Lei, C. Evaluation of the shear adhesion strength of impact ice by a new method. *Eng. Fract. Mech.* **2023**, *292*, 109641. [[CrossRef](#)]
29. Sarkar, D.K.; Farzaneh, M. Superhydrophobic Coatings with Reduced Ice Adhesion. *J. Adhes. Sci. Technol.* **2009**, *23*, 1215–1237. [[CrossRef](#)]
30. Javan-Mashmool, M.; Volat, C.; Farzaneh, M. A new method for measuring ice adhesion strength at an ice–substrate interface. *Hydrol. Process.* **2010**, *20*, 645–655. [[CrossRef](#)]
31. Davis, A.; Yeong, Y.H.; Steele, A.; Bayer, I.S.; Loth, E. Superhydrophobic Nanocomposite Surface Topography and Ice Adhesion. *ACS Appl. Mater. Interfaces* **2014**, *6*, 9272–9279. [[CrossRef](#)] [[PubMed](#)]
32. Zhang, Y.; Chen, L.; Liu, H. Study on ice adhesion of composite anti-/deicing component under heating condition. *Adv. Compos. Lett.* **2020**, *29*, 2633366X20912440. [[CrossRef](#)]

**Disclaimer/Publisher's Note:** The statements, opinions and data contained in all publications are solely those of the individual author(s) and contributor(s) and not of MDPI and/or the editor(s). MDPI and/or the editor(s) disclaim responsibility for any injury to people or property resulting from any ideas, methods, instructions or products referred to in the content.